Biochimica et Biophysica Acta, 664 (1981) 201–210
Elsevier/North-Holland Biomedical Press

BBA 79248

PERMEABILITY TO IONS OF BOVINE RETINAL DISK MEMBRANE VESICLES IN THE BLEACHED STATE

ERIC J. AMIS, DAN J. WENDT, EDWARD D. ERICKSON and HYUK YU *

Department of Chemistry, University of Wisconsin, 1101 University Avenue, Madison, WI 53706 (U.S.A.)

(Received October 13th, 1980)

Key words: Ion permeability; Bleaching; Light scattering; (Rod outer segment)

The permeability of the bleached disk membrane of retinal rod outer segments to univalent and divalent ions is studied by light scattering. The membranes are isolated from frozen dark-adapted bovine retinae, swollen into spherical vesicles in a hypotonic medium and bleached in dilute suspension and their size is determined by elastic and quasi-elastic light scatterings. Various electrolytes are then added to the suspending medium in order to examine their osmotic activity relative to the vesicles deformation characteristics. By following the deformation behavior of the membrane vesicles by elastic light scattering in terms of the oblate ellipsoidal shell model, the osmotic activity of a given electrolyte is qualitatively deduced and thereby the permeability of the membrane to the electrolyte is ranked in reference to a chosen standard, i.e., sucrose. By this method, we show that the permeabilities to Na^+, K^+, Mg^{2+} and Ca^{2+} are all alike, and those to halides (F^-, Cl^-, Br^-, I^-), nitrate and phosphates ($HPO_4^{2-}/H_2PO_4^-$) are similar. Acetate, however, is about 3-times more permeative, while sulfate is less permeative than the other anions by about the same factor. The viability of our method is checked with use of an ionophore, lasolocid (X-537A), by establishing partial recovery from the osmotic deformation through the suppression of the cation osmotic effect. Ion-induced aggregation and pH-dependent size and shape changes are both found to be insignificant.

Introduction

The visual cycle is initiated at the photopigment, rhodopsin, on the disk membranes of rod outer segments of vertebrate retinae. Structurally as well as functionally, rhodopsin is such an integral part of the disk membranes that the membranes should be regarded as photoreceptor surfaces for scotopic vision [1]. Irrespective of whether the photoreceptor function of the disk membranes will eventually turn out to require Ca^{2+} [2] as the transmitter substance or cyclic GMP [3] as the mediator for protein dephosphorylation of Na^+ gates on the plasma membrane, there appears to be no question as to the importance of photoinduced ion transport across the disk membranes. In particular, one may ask, in the context of the model of Hagins and Yoshikami [4]: is the bleached membrane more permeable to Ca^{2+} than other physiological cations? If not, is the Ca^{2+} efflux counter-balanced by an influx of other cations so as to maintain the intravesicular osmolarity constant? With these and similar questions in mind, we set out to examine the permeability of the membrane in the bleached state to sodium, potassium, magnesium and calcium ions. For the sake of completeness we have also examined halides, phosphates, nitrate, sulfate and acetate with Na^+ as the common cation. This is to report our findings of the permeabilities to these ions.

Since the disk membranes are known to respond to an osmotic gradient in the native rod outer segment as well as in the vesicular form [5–11], one can

* To whom correspondence should be addressed.

probe the permeability to individual ions by observing how the vesicles deform with different concentrations of a given ion in the suspending medium. If a given solute is completely permeative to the vesicles, there should exist no chemical potential gradient across the membrane bilayer and the vesicles should remain undeformed, independent of solute concentration. On the other hand, if the membrane is totally impermeable to a solute, addition of that solute to the suspending medium will induce transport of components to which the membrane is permeable, principally water, until the equilibrium is established in which the residual chemical potential gradients are counter-balanced by the membrane stiffness. In other words, the vesicles will act as semi-permeable membranes whereby water and other permeating components drain out of the vesicles within a certain limit; and that limit is controlled by the membrane stiffness. As the draining proceeds the surface area of the vesicle must decrease until the elastic free energy arising from the lateral compressibility of the membrane is counteracted by the gradient of chemical potential across the membrane. Thus one should be able to test the permeability of the membrane to different ions under a plausible assumption that the ions do not affect the membrane stiffness differently. If so, the vesicle deformation profile vis-a-vis the concentration of the test ions can be used to rank the permeability, provided a common counter ion is used to maintain the contribution of its chemical potential gradient at a constant level.

The methodology for determining the vesicle deformation at different ionic concentrations is the same as that used earlier with a relatively impermeative non-electrolyte, sucrose [11]. This is to combine angular dependence of elastic light scattering (total intensity scattering) with quasi-elastic light scattering to effect the two-parameter characterization of the membrane vesicles in terms of an oblate ellipsoidal shell model. Unlike the case of sucrose, however, here we are interested in the qualitative trend of how different series of ions affect the osmotic deformation of the vesicle such that the two-parameter characterization need not be effected as quantitatively as before. Our focus is on a serial ranking of the permeability to each set of cations and anions with use of the two techniques.

As to the appropriateness of the vesicle system that we have studied, one could reasonably question whether what we have examined has any bearing on the properties of disk membranes in vivo since our suspending media (1–20 mosM) are so hypotonic that they can scarcely simulate the native cytoplasm (approx. 250 mosM); hence the properties should be quite different. Our response to that question is as follows. To the extent that the vesicles extracted from frozen and dark-adapted retinae have been shown to preserve the same sidedness [12], photopigment content [13] and possibly surface area [9], they may be regarded as intact native disks in terms of their intramembranous constitution. If so, the permeability of the vesicles may plausibly be regarded as unaltered from that of the native disks in rod outer segments. On the other hand, a recent report by Uhl et al. [14] suggests that the freshness of a membrane preparation is crucial in preserving the low proton permeability in the unbleached state. If we had a protocol to assay the freshness of a membrane preparation, this suggestion could well be tested with our disk vesicle preparations. Unfortunately, we know of no such protocol. This state of affairs is, in our opinion, a major stumbling block in any interlaboratory comparison of disk membrane preparations relative to their permeability characteristics. Though we could have inflicted functional damage to the disks, the integrity of photopigment appears intact as judged by the absorbance ratio A_{278}/A_{498} (see below). Thus it is hoped that what we observe with the vesicles is in some way indicative of the in vivo disk permeability properties. At worst, we have studied a model membrane derived from the disks. The main reason for the use of swollen vesicles instead of disks in isotonic media is that we can amplify the osmotic deformation so as to enhance the data precision, hence to apply effectively the experimental techniques employed here.

Materials

With the following modification, bovine rod outer segment disk membranes were isolated from frozen retinae (American Stores Packing Co.) by the method of Smith et al. [15] as previously detailed [10]. For the purpose of bursting rods to release the swollen disks, 3% or 5% aqueous Ficoll (molecular weight 400 000; Sigma) was used. The more rigorous separa-

tion by 3% Ficoll produced better disk fractions as judged by the A_{278}/A_{498} ratio; the ratio was found in the range 1.9 ± 0.2 instead of 2.5 ± 0.2 for previous preparations using 5% Ficoll floatations. Improved quality of the elastic light scattering profiles (see below) was also observed indicating better homogeneity of the vesicle suspensions.

The control suspending medium was 1 mM imidazole buffer, pH 6.9, and all suspensions were bubbled with Argon and filtered through a 5 μm Teflon filter (Millipore or Gelman) prior to the light scattering measurements.

Methods

Elastic light scattering

After removing the unbleached disk membranes from the Ficoll floatation, they were in most cases suspended and washed in the particular ionic solution in which the elastic light scattering measurement was to be carried out. The final suspension of membranes was made such that after filtration the concentration was about $3 \cdot 10^9$ vesicles/ml as determined by A_{633} [13]. At this point the membrane suspensions were bleached and the elastic light scattering profile over the range of scattering angle from 30° to 150° was measured at 2° increments. Light scattering measurements were performed using a SOFICA Photogoniometer (Bausch and Lomb; Model 40 000) interfaced through an analog-to-digital converter (Datel ADCHX12BGC) to an Apple II microcomputer (Apple Computer Inc., Cupertino, CA) with video display and floppy disk storage. The incident green light (546 nm) and scattered light were vertically polarized. Because of the extremely large size of the scattering particles no background scattering corrections were necessary. Also, over the range of concentration $8 \cdot 10^8$–$1 \cdot 10^{10}$ vesicles/ml, no concentration dependence of the scattering profile was observed.

As we have previously done in the case of sucrose [11], the elastic scattering results are plotted as $\sin^2(\theta/2)I_{vv}(\theta)$ vs. $\sin(\theta/2)$ where θ is the scattering angle and $I_{vv}(\theta)$ is the polarized scattering intensity. The profiles of such plots are interpreted in terms of the oblate ellipsoidal shell model. In the experiments where the ionophore (lasalocid) was used, incubation time and concentrations were carefully optimized. In the experiments without ionophore, time dependence was found to be negligible within about 4 h beyond which we found gradual disappearance of the undulation amplitude, indicating vesicle degradation and/or aggregation.

Quasi-elastic light scattering

Suspensions prepared in an identical manner as the elastic light scattering suspensions were used for the measurement of the translational diffusion coefficient by quasi-elastic light scattering. The detection and analysis of the scattered intensity were effected by means of the photon count autocorrelation method [16]. A 64 channel real time autocorrelator (Malvern K7025; Malvern Instruments, Ltd., Malvern, Worcs., U.K.) connected to a commercial goniometer (Malvern RR103) was used to measure the characteristic decay constant of the photocurrent autocorrelation arising from the homodyne quasi-elastic scattering. The normalized autocorrelation function in terms of a single decay constant Γ is expressed as

$$g(\tau) = 1 + Ae^{-2\Gamma\tau} \tag{1}$$

with

$$\Gamma = D\kappa^2 \tag{2}$$

where A is an instrument optical constant, D the translational diffusion coefficient and κ the magnitude of the scattering wave vector, defined as $(4\pi n/\lambda_0)\sin(\theta/2)$ with n being the refractive index of the medium, λ_0 the incident wave length in vacuo and θ the scattering angle. The correlator was interfaced to an Apple II microcomputer allowing data display, data storage and iterative least-squares fitting of the exponential autocorrelation function. Analysis of the decay constant was performed over a scattering angle range from 22° to 135°, and the translational diffusion coefficient D was deduced from the angular dependence of the decay constant via Eqn. 2. Both an unpolarized He/Ne laser (3 mW, 632.8 nm, Spectra Physics) and a polarized Ar laser (200 mW, 514.5 nm, Lexel Model 75-.2) were used for these experiments.

Results and Discussion

In Fig. 1 is displayed the elastic light scattering profiles of the vesicles in NaCl, KCl, $MgCl_2$, and

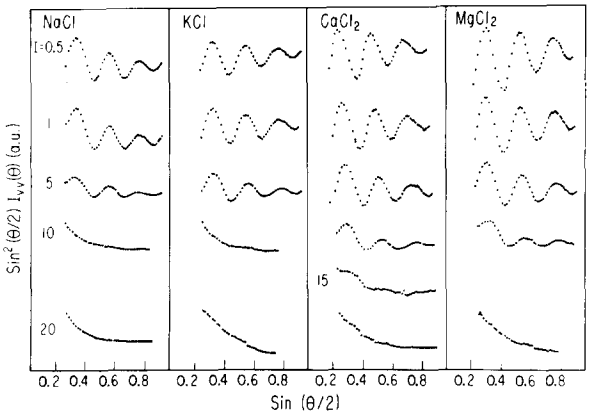

Fig. 1. Angular dependence of elastic light scattering, $\sin^2(\theta/2)I_{VV}(\theta)$ vs. $\sin(\theta/2)$, for the chlorides of Na, K, Mg and Ca in 1 mM imidazole at total ionic strengths of 0.5, 1, 5, 10 (15 for Ca^{2+}) and 20 mM.

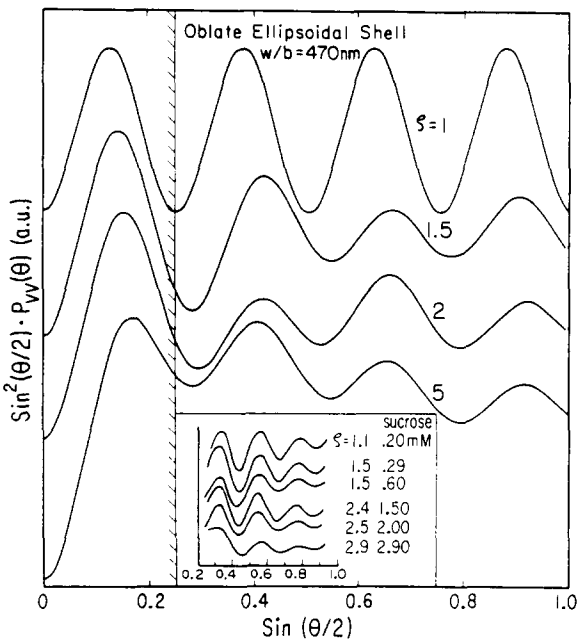

Fig. 2. Theoretical plots of scattering function $\sin^2(\theta/2)P_{VV}(\theta)$ vs. $\sin(\theta/2)$ of oblate ellipsoid shell at indicated values of the axial ratio is shown for $n = 1.333$; $\lambda_0 = 546$ nm; $b = 470$ nm. The inset shows experimental profiles for sucrose from Ref. 11.

$CaCl_2$ at different concentrations, expressed in ionic strength units. It is evident that the profiles are rather similar for each set of electrolytes, i.e., NaCl and KCl (uni-univalent) and $MgCl_2$ and $CaCl_2$ (di-univalent), relative to the damping progression of the undulation amplitude with increasing ionic strength. It should be noted that in terms of osmolarity (assuming ideality in the mM range), uni-univalent electrolytes cover a 2–40 mosM range while di-univalent electrolytes span a 0.33–6.67 mosM range. The apparent difference in the progression of scattering profiles with respect to ionic strength therefore disappears when the comparison is made on the basis of total (ideal) osmolarity. We shall return to this point later. For now we concentrate on qualitative features of these scattering profiles. In order to extract the significance of the scattering profiles, we show in Fig. 2 the theoretical profiles of the oblate ellipsoidal shell model calculated for a semi-major axis of 470 nm at varying axial ratios [17]. In the inset, we display the observed scattering profiles of the vesicles in different osmolarities of sucrose [11]. The axial ratios, ρ, indicated in the figure, are determined by combination of elastic and quasi-elastic light scatterings. The general trend of damping progression of the undulation amplitude with increasing ρ value is readily seen. Hence, if our purpose is to rank various cations relative to their permittivity through the vesicles, then the undulation amplitude alone should provide a qualitative measure of the vesicle deformation provided the semi-major axis does not change.

It has been shown earlier that the semi-major axis b does not change with osmolarity of sucrose while the vesicles deform by increasing the eccentricity of the oblate shell. A similar behavior of the vesicle deformation might be expected with electrolytes. The results in Fig. 1 can be used to establish this point as follows. The extrema position of the scattering profiles is an inverse linear function of the semi-major axis, b, within relatively narrow windows, at all values of the axial ratio ρ. This is demonstrated in Fig. 3, where the theoretically calculated extrema positions from the first-order minimum to the fifth-order minimum are plotted against ρ. The widest window is the third-order minimum, which is no more than 9% wide between $\rho = 1$ and $\rho = 1.6$. Thus the insensitivity of the extrema position is amply demonstrated. The results in Fig. 1 show clearly that the extrema positions are well preserved at different ionic concentrations for all four electrolytes. We therefore conclude

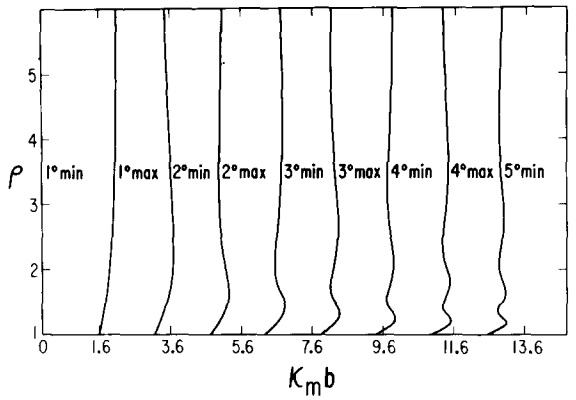

Fig. 3. The theoretical extrema positions of the scattering profiles of oblate ellipsoidal shell, calculated from the scattering form factor given in Ref. 11. These plots show that the extrema in the scattering profile plots, given by $\sin^2(\theta/2)I_{VV}(\theta)$ vs. $\sin(\theta/2)$, are an inverse linear function of the semi-major axis b within narrow windows for any value of the axial ratio ρ, where κ_m stands for the magnitude of scattering wave vector at a given extrema position.

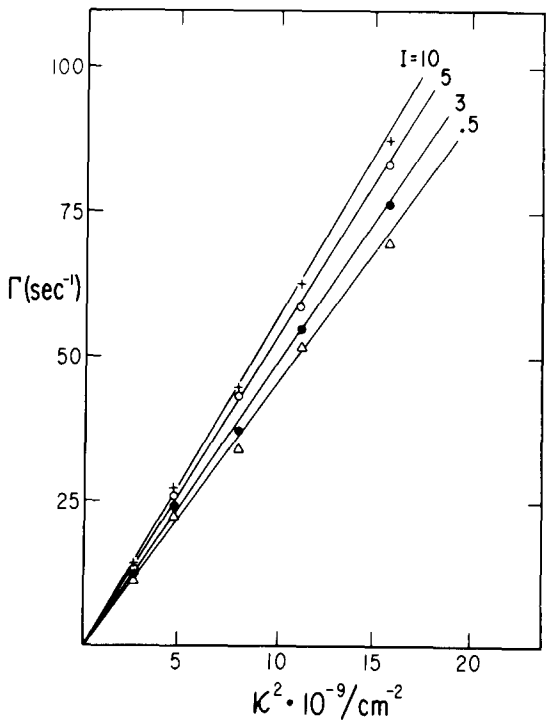

Fig. 4. The decay constant Γ of the single exponential correlation function of the quasi-elastically scattered light is plotted against the square of the scattering wave vector κ. The slope is the diffusion coefficient. The numbers indicate the total ionic strength in mM of the suspending medium, 1 mM imidazole, pH 7, in various NaCl concentrations.

that the semi-major axis b is conserved at different ionic concentrations. Having thus established that b does not change with ionic concentration, the observed progressive attenuation of the undulation amplitude with increasing ionic concentration is ascribed to the increasing axial ratio ρ of the vesicles.

Before we can draw the final conclusion from this set of measurements shown in Fig. 1, we need to dispose of two likely complications. The first is ion-induced aggregation and the second is the pH effect. We shall now show how we eliminate both of them. The observed attenuation of the undulation amplitude could equally be ascribed to ion-induced vesicle aggregation, resulting in broader distributions of vesicle sizes as ion concentrations are increased. This, however, is readily ruled out by performing the quasi-elastic light scattering measurements with the same set of NaCl concentrations as used in the elastic light scattering experiment and demonstrating that the translational diffusion coefficient increases with ion concentration. The results are displayed in Fig. 4. The translational diffusion coefficient D of oblate ellipsoids as given by Perrin [18] is

$$D = \frac{kT}{6\pi\eta b}\,\rho G(\rho) \tag{3}$$

with

$$G(\rho) = \frac{\tan^{-1}(\rho^2 - 1)^{1/2}}{(\rho^2 - 1)^{1/2}} \tag{4}$$

where η is the viscosity of the suspension, b is the semi-major axis, and kT has the usual meaning. The term $\rho G(\rho)$ is a monotonically increasing function of ρ, hence D should also increase monotonically with ρ when b remains constant. Fig. 4 gives a clear demonstration of this trend. Had aggregation been principally responsible for attenuating the undulation amplitude of the scattering profiles, we should have observed the opposite trend, namely that D should decrease with NaCl concentration. In terms of Perrin's equation, we can quantify the results in Fig. 4 by determining the axial ratio. If we take the D value in 1 mM imidazole ($I = 0.5$ mM) as the reference

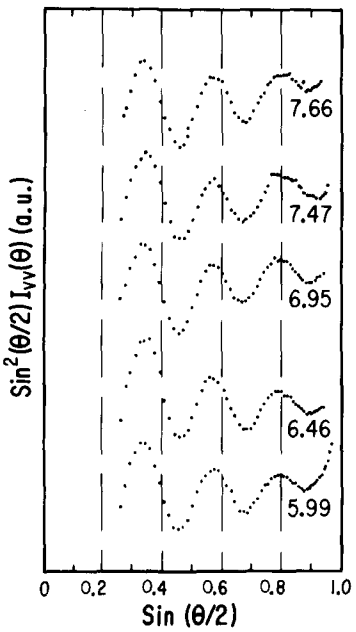

Fig. 5. Elastic light scattering profiles of disk membrane vesicle suspensions in imidazole at a total osmolarity of 2 mM. pH values are as indicated.

spherical shell state, i.e., $D = 4.52 \cdot 10^{-9}$ cm^2/s, Stokes' radius 470 nm, then the ρ values computed for the other ion concentrations are 1.3 at 3 mM, 1.8 at 5 mM and 2.3 at 10 mM. These values should be compared with those listed in the inset of Fig. 2 where ρ changes from 1.1 to 2.9 when the sucrose concentration is increased from 0.2 mM to 2.9 mM. If we hypothesize that the vesicle deformation is solely due to the osmolarity of impermeative solutes and that sucrose is such a solute [19], then it requires about 2 mosM sucrose to induce the same extent of vesicle deformation, $\rho = 2$, as with 10 mM NaCl. This is a remarkable comparison in terms of the permittivities of Na^+ and Cl^- relative to that of sucrose, since the ideal osmolarity of 10 mM NaCl should be 20 mosM.

We next examine the sensitivity of the vesicle shape and size to the pH of the suspending medium in order to eliminate spurious pH effects on the vesicle deformation (each suspension undergoes a slight pH change due to the additional buffering action of the vesicles). With the use of imidazole, HCl and NaCl we change the pH of the suspension between 6.0 and 7.8 at a constant ionic strength of 2 mM. The elastic scattering profiles of the vesicles are shown in Fig. 5. It is clear that in the pH range examined, the vesicle size and shape remain the same.

Having thus eliminated any aggregation and pH effect, we can now turn to comparison of the four ions Na^+, K^+, Ca^{2+} and Mg^{2+}. In order to observe the osmotic effect of these four, we should compare the scattering profiles at a given concentration of both cation and anion if they are equally active. If, on the other hand, the chloride ion is far more permeating than the cations, then one should compare profiles at differing cation molar concentrations. In terms of ideal osmolarity, NaCl and KCl are about twice that of $MgCl_2$ and $CaCl_2$ at a given ionic strength. For instance, at 5 mM total ionic strength (including the

TABLE I

CONCENTRATION AND TOTAL OSMOLARITY OF BUFFER AND ELECTROLYTES AT DIFFERENT IONIC STRENGTHS

Figures are presented in units of mM. IMDZL, imidazole; $IMDZL^+$, imidazolium ion.

Total ionic strength	MCl				MCl_2			
	IMDZL/ $IMDZL^+$	Cl^-	M^+	osM	IMDZL/ $IMDZL^+$	Cl^-	M^{2+}	osM
0.5	1.0	0.5	–	1.5	1.0	0.5	–	1.5
1	1.0	1.0	0.5	2.5	1.0	0.83	0.17	2.0
5	1.0	5.0	4.5	10.5	1.0	3.5	1.5	6.0
10	1.0	10.0	9.5	20.5	1.0	6.34	3.17	11.0
15	1.0	15.0	14.5	30.5	1.0	10.16	4.83	16.0
20	1.0	20.0	19.5	40.5	1.0	13.5	6.5	21.0

contribution from imidazole) the total osmolarity for NaCl and KCl is 10.5 mosM whereas it is 6 mosM for $MgCl_2$ and $CaCl_2$. These values are listed in Table I. By comparing the scattering profiles for the solutions with the four cations we see that in 10 mM ionic strength $MgCl_2$ and $CaCl_2$ the vesicles show a similar deformation as in 5 mM NaCl and KCl. We can also see that for Ca^{2+} and Mg^{2+} the profiles are not completely damped out until 20 mM ionic strength is reached as compared to 10 mM for the Na^+ and K^+. It should be noted that the total osmolarity of the divalent cation-chloride at 20 mM ionic strength is 21 mosM, while that of the univalent cation-chloride at 10 mM ionic strength is 20.5 mosM. Hence, the complete damping of the undulation amplitude is reached at about 20 mosM, and such a threshold is independent of the valency of the cations. This observation has prompted us to compare the progressive attenuation of the undulation amplitude in all four electrolytes as a function of total osmolarity instead of ionic strength. The results show that there is no difference among the four electrolytes. The similar appearance of the scattering profiles in NaCl and KCl at $I = 5$ mM and in $MgCl_2$ and $CaCl_2$ at $I = 10$ mM shown in Fig. 1, attests to this point. Thus, we arrive at the conclusion that the osmotic activities of Na^+, K^+, Ca^{2+}, Mg^{2+}, and Cl^-, relative to inducing the osmotic deformation of disk membrane vesicles, are about the same. We should add parenthetically here that it is not a priori obvious that the nonspecific membrane permeability relative to different ions is purely osmotic in nature. It could very well be controlled by the interfacial potential, i.e., electrostatic in nature, such that the ionic strength of similarly permeating ions should be the relevant independent variable instead of the osmolarity because the Debye-Hückel screening length controlled by ionic strength affects the interfacial potential such as the Guoy-Chapman electrical double layer [20]. Hence, we first picked the ionic strength as a trial variable in order to examine its effect on the vesicle deformation. As it turns out, any effect of ionic strength is dwarfed by the osmotic gradient as the controlling factor.

The results outlined above indicate that the permeability to these ions of the bleached disk membranes are indistinguishable, and certainly there appears to be no unique permeability to Ca^{2+} compared with that of Na^+, K^+, and Mg^{2+}. In terms of the Hagins-Yoshikami model, one might have expected that Ca^{2+} is significantly more permeative than the rest. Non-uniqueness of Ca^{2+} permittivity, however, does not constitute sufficient evidence contrary to the calcium transmitter model; Ca^{2+} may be the only permeable cation present in the intradiskal space in significant amount, which is effluxed by photoexcitation.

Before closing this part of the discussion, we present the results of another set of experiments which provide a further verification of our analysis scheme. The experiments are designed to render the cations permeable with the aid of an ionophore, lasalocid, and to examine the resulting scattering profiles vis-a-vis those without the ionophore. Lasalocid is known to be an excellent ionophore for univalent and divalent cations [21]. If we assume that lasalocid is so efficacious in transporting these cations that its presence in the suspending media completely abolishes the osmotic effect contributed by the cations, then we should expect the following effective osmolarity at $I = 10$ mM in the two types of electrolyte: 20.5 mosM and 10 mosM in MCl without and with lasalocid, respectively, and 11 mosM and 6.34 mosM in MCl_2 without and with lasalocid, respectively (see Table I). In such ideal circumstances, we then expect the scattering profiles with lasalocid in 10 mM MCl to resemble those without lasalocid in MCl at $I = 5$ mM or in MCl_2 at $I = 10$ mM. The profiles with lasalocid in 10 mM MCl_2 should resemble those in MCl at $I \approx 3$ mM or in MCl_2 at $I = 5$ mM without lasalocid. The results are displayed in Fig. 6. In the top profile, a partial recovery of the deformation is rather dramatically shown in the case of Na^+ at 10 mM; the profile with lasalocid seems to resemble the one in $I = 5$ mM without lasalocid. Though it may turn out to be fortuitous, the result seems to confirm our expectation in the best possible circumstances. Results with divalent cations are also consistent with the expectations outlined above. At 10 mM ionic strength in $MgCl_2$ and $CaCl_2$, the total osmolarity is 11 mosM so that the profiles without ionophore are about the same as those in NaCl and KCl at $I = 5$ mM. The chloride contributes 6.3 mosM while divalent cations contribute 3.2 mosM, so the ionophore at the very best circumstance can abolish only the osmotic effect of 3.2 mosM of cations thus making insignificant difference in the profiles. Indeed, such seems to be the case in

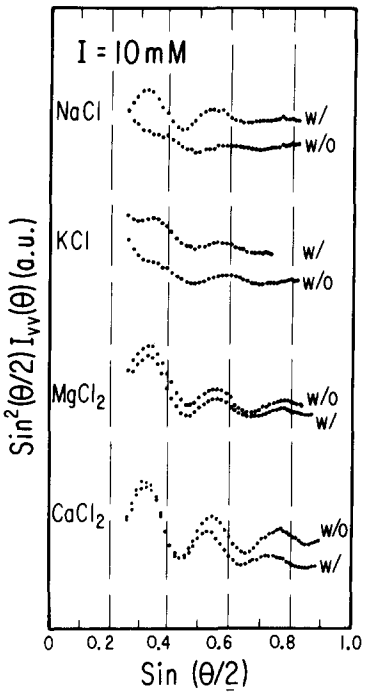

Fig. 6. Light scattering profiles for rod outer segment suspensions in NaCl, KCl, $MgCl_2$ and $CaCl_2$ with and without addition of ionophore lasalocid.

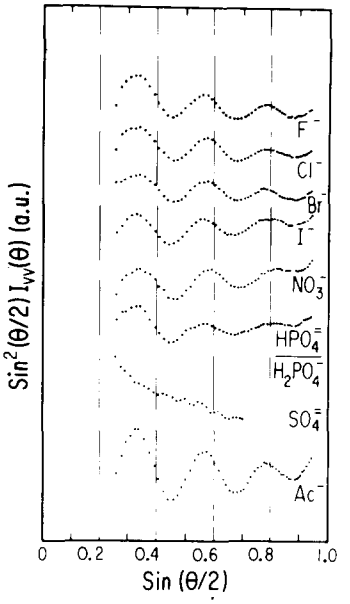

Fig. 7. Light scattering profiles in 6 mM osmolarity with different anions and Na^+ as the common cation. Effect of anions at pH 7.

the bottom two profiles in Fig. 6. The situation in KCl is less clearcut and we have no explanation to account for the difference between Na^+ and K^+. It may be noted here that Uhl et al. [14] find in the unbleached state a considerable K^+ permeability, which can be abolished by mM amounts of divalent cations, while no measurable permeability is found with Na^+, Ca^{2+}, and Mg^{2+}. Whether the difference between their results and ours could solely be due to the photochemical state or in part due to membrane freshness must be settled in the future.

A similar experiment comparing different anions has been performed. In this case, using Na^+ as the common cation, at pH 7 and an ideal osmolarity of 6 mosM, we show in Fig. 7 a comparison of halides, nitrates, $HPO_4^{2-}/H_2PO_4^-$, SO_4^{2-} and Ac^-. The first four are very similar despite a wide range of ionic radii. Nitrate and phosphate also appear to produce the same effect although they are no longer simple atomic ions. The interesting cases are those of sulfate and acetate where striking differences are observed. Sulfate at 6 mosM causes the elastic scattering profile to resemble the sodium chloride profile at more than 3-times the osmolarity, i.e., 10 mM ionic strength. Quasi-elastic light scattering results (not shown here) confirm that, as in the case of NaCl, we are indeed observing an ellipsoidal deformation and not aggregation. While this indicates that the membrane is considerably less permeable to sulfate than to the other ions studied, it is still more permeable than to sucrose as described previously (again there is about a factor of three in the concentrations required to cause the same deformation).

Turning to acetate, the opposite trend is observed. Here we see the effect of deformations which are perhaps only half that expected. This can be seen in Fig. 8 where sodium acetate and sodium chloride at 5 and 10 mM ionic strength are shown. Clearly the membranes are more permeable to acetate than to chloride, and in fact in 10 mM NaAc the profile is comparable to that in 5 mM NaCl. A complete concentration series for acetate is shown in Fig. 9. If we postulate that the membrane is completely permeable to acetate, then the results in Fig. 9 are consistent with the osmotic effect caused by Na^+ alone. It should be

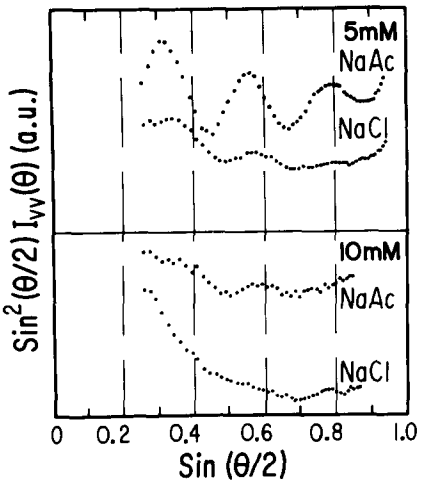

Fig. 8. Light scattering profiles in sodium acetate and sodium chloride at the indicated ionic strengths.

noted that acetate is the only organic anion that we have examined. The amphoteric character of an organic anion by virtue of its hydrophilic ion on the one end and hydrophobic group on the other end could allow it to easily permeate the membrane bilayer. If this is true, an aliphatic alcohol may also be able to permeate and behavior similar to that of acetate would be expected for ethanol, a non-ionic analog of the acetate ion. With ethanol, we indeed have observed that it has no osmotic effect on the vesicles up to 150 mM. In fact, ethanol is the most inefficacious compound that we have tested relative to osmotic deformation. On the other hand, a disaccharide, sucrose, is the most effective in producing the osmotic deformation.

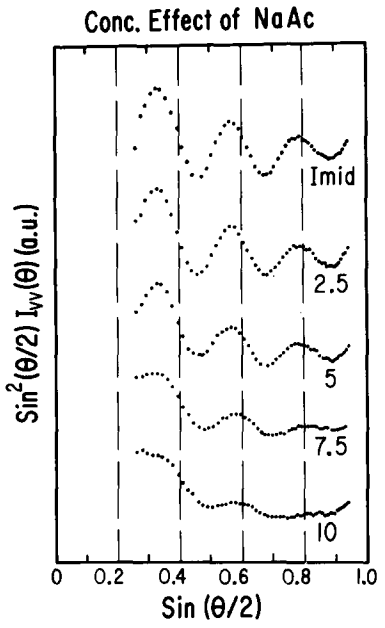

Fig. 9. Light scattering profiles in sodium acetate with various ionic strengths as indicated.

In summary, we have shown that the osmotic response of the disk membrane vesicles could be used to probe their ionic permeability with a combination of elastic and quasi-elastic light scattering techniques. In the case of the bleached membranes, we have established that permeability to Ca^{2+} is not singular as compared to Na^+, K^+, Mg^{2+}, halides, nitrates and phosphates. Acetate and sulfate however are different from the other anions.

Acknowledgments

This is supported in part by an NIH grant, EY01483 and by the Biomedical Research Support Grant of NIH administered through the Graduate School of the University of Wisconsin-Madison. We are indebted to Dr. Edwin M. Turner for his assistance in interfacing the autocorrelator to the Apple II microcomputer and to Mr. Taihyun Chang in generating the computation results of Fig. 3. We also gratefully acknowledge the generous gift of X-537A from Dr. W.E. Scott of Hoffman-LaRoche.

References

1 Field, J., Magoun, H. and Hall, V. (1959) Handbook of Physiology, Vol. 1, American Physiological Association, Washington, DC
2 Hagins, W.A. (1972) Annu. Rev. Biophys. Bioeng. 1, 131–158
3 Hubbell, W.L. and Bownds, M.D. (1979) Annu. Rev. Neurosci. 2, 17–34
4 Hagins, W.A. and Yoshikami, S. (1974) Exp. Eye Res. 18, 299–305
5 Heller, J., Ostwald, T.J. and Bok, D. (1971) J. Cell Biol. 48, 633–649
6 McConnell, D.G. (1975) J. Biol. Chem. 250, 1898–1906
7 Korenbrot, J.I., Brown, D.T. and Cone, R.A. (1973) J. Cell Biol. 56, 389–398
8 Hoffman, W.F., Norisuye, T. and Yu, H. (1977) Biochemistry 16, 1273–1278

9 Raubach, R.A., Nemes, P.P. and Dratz, E.A. (1974) Exp. Eye Res. 18, 1–12
10 Norisuye, T., Hoffman, W.F. and Yu, H. (1976) Biochemistry 15, 5678–5682
11 Norisuye, T. and Yu, H. (1977) Biochim. Biophys. Acta 471, 436–452
12 Adams, A.J., Tanaka, M. and Shichi, H. (1978) Exp. Eye Res. 27, 595–605
13 Amis, E.J., Davenport, D.A. and Yu, H. (1981) Anal. Biochem., in the press
14 Uhl, R., Kuras, P.V., Anderson, K. and Abrahamson, E.W. (1980) Biochim. Biophys. Acta 601, 462–477
15 Smith, H.G., Jr., Stubbs, G.W. and Litman, B.J. (1975) Exp. Eye Res. 20, 211–217
16 Berne, B.J. and Pecora, R. (1976) Dynamic Light Scattering, Wiley-Interscience, New York, NY
17 Yu, H. (1981) Methods Enzymol., in the press
18 Perrin, F. (1936) J. Phys. Radium 7, 1–11
19 Darszon, A., Montal, M. and Zarco, J. (1977) Biochem. Biophys. Res. Commun. 76, 820–827
20 Träuble, H., Teubner, M., Woolley, P. and Eibl, H. (1976) Biophys. Chem. 4, 319–342
21 Pressman, B.C. (1976) Annu. Rev. Biochem. 45, 501–530